

# Multi-fractal Behaviors of Relative Humidity over China

GAO Li-Hao<sup>1,2</sup> and FU Zun-Tao<sup>1</sup>

<sup>1</sup> Department of Atmospheric and Oceanic Sciences & Laboratory for Climate and Ocean-Atmosphere Studies, School of Physics, Peking University, Beijing 100871, China

<sup>2</sup> Key Laboratory of Regional Climate-Environment for Temperate East Asia, Institute of Atmospheric Physics, Chinese Academy of Sciences, Beijing 100029, China

Received 30 March 2012; revised 17 May 2012; accepted 14 June 2012; published 16 March 2013

**Abstract** The multi-fractal behaviors of relative humidity over China are studied using the multi-fractal detrended fluctuation analysis (DFA) method. Three multi-fractal parameters (the spectrum width  $\Delta\alpha$ , the asymmetry  $\Delta\alpha_{as}$ , and the long-range correlation exponent  $\alpha_0$ ) of the singularity spectrum are introduced to quantify the multi-fractal behaviors. The results show that multi-fractality exists in daily humidity records over most stations in China and is mainly due to the broad distribution of the probability density of the sequence values. Strong multi-fractal behaviors over some stations in the Yunnan, Guangdong, and Inner Mongolia provinces are obvious. These behaviors are mainly caused by different long-range correlations between large and small fluctuations. The asymmetry of the singularity of relative humidity records is weak, except for a small number of stations in the far east and west of China, where the singularity spectrum is left-skewed. Finally, the long-range correlations in North China are stronger than those in South China, which indicates better predictability in North China. By studying the parameters of the multi-fractal spectrum, various data of long-range power law correlations of the relative humidity records are obtained, which may provide theoretical support for climate prediction.

**Keywords:** long-range correlation, scaling exponent, multi-fractal, multi-fractal detrended fluctuation analysis

**Citation:** Gao, L.-H., and Z.-T. Fu, 2013: Multi-fractal behaviors of relative humidity over China, *Atmos. Oceanic Sci. Lett.*, **6**, 74–78.

## 1 Introduction

There are various processes of different temporal-spatial scales in climate systems. These processes can be recorded in observational series, which can be used to study the dynamical processes. Recently, researchers have found that fluctuations of different time scales in these series exhibit self-similar structures, and this kind of self-similarity can be quantified by defining the scaling exponent for the existing scale invariance. For example, the detrended fluctuation analysis (DFA) function shows power-law variations with increasing time scales, which reflect the long-range correlations of a time series (Koscielny-Bunde et al., 1998; Talkner and Weber, 2000; Kantelhardt et al., 2001; Bunde and Havlin, 2002;

Fraedrich and Blender, 2003; Liu, 1990; Shi et al., 2005). For many observational records, however, including the relative humidity records we used in the study, a single scaling exponent is not sufficient to fully characterize the records' long-term correlations. The single scaling exponent only characterizes the long-range correlations of certain fluctuations of the whole records, and thus, more scaling exponents are needed to fully characterize the records' long-range correlation features, although some of these exponents may be close (Jiang and Deng, 2004; Guo et al., 2004; Chen and Guo, 1997; Feng et al., 2010) each other. The singularity spectrum can be employed to describe the range, strength, and asymmetry of the multi-scaling exponents, which reflect the records' multi-fractal behaviors (Kantelhardt et al., 2002).

Relative humidity is an important climatic variable that has a direct effect on precipitation, and thus, it is necessary to study the law of humidity variation, as it is related to the future drought-wet changes. The single scaling behavior of relative humidity was studied by researchers (Vattay and Harnos, 1994; Lin et al., 2007; Chen et al., 2007) who investigated the long-term power law correlation of the relative humidity records, to some extent. More comprehensive studies from a multi-fractal view are still needed to better understand the totality of the scaling behaviors. Multi-fractal detrended fluctuation analysis (MF-DFA) (Kantelhardt et al., 2002), as an easily programmable method suitable for studying the multi-fractal properties of non-stationary time series, has been favored by researchers. We employed this method to study the multi-fractal behaviors of relative humidity over China. This study provides further information about relative humidity variations and is helpful to study future climate changes.

## 2 Data and methodology

Daily mean relative humidity records were obtained from a high-quality daily surface climate data set processed by Chinese National Meteorological Information Center (NMIC) of 194 Chinese meteorological stations taking part in an international exchange. This data set has been used to study climate changes over China in recent years (Zhai and Pan, 2003; Zou et al., 2005; Zhai et al., 2004). In this study, three records were removed for their short data length. The remaining records have a length of approximately 50 years from 1951 to 2000.

The main procedures of the MF-DFA method include the five steps below (Kantelhardt et al., 2002):

Step 1: Calculate the profile by integrating observational series ( $x_i$ ),

$$Y_i = \sum_{k=1}^i (x_k - \bar{x}), \quad (1)$$

where  $\bar{x} = \frac{1}{N} \sum_{i=1}^N x_i$  ( $N$  is data length).

Step 2: Divide the profile ( $Y_i$ ) into  $N_s = [N/s]$  nonoverlapping segments of equal length  $s$ . The same procedure is repeated from the beginning of the opposite side to include the remainder of the series because  $N$  is not always an integral multiple of segment length  $s$ . Then, additional  $N_s$  segments of length  $s$  are obtained.

Step 3: Detrend the profile for every segment by subtracting local trend  $P_\nu(j)$  for  $2N_s$  segments to obtain the detrended profile,

$$y_\nu(j) = Y_\nu(j) - P_\nu(j) \quad (\nu = 1, \dots, 2N_s, j = 1, \dots, s). \quad (2)$$

The corresponding variance function is given by

$$F^2(\nu, s) = \frac{1}{s} \sum_{j=1}^s (y_\nu(j))^2 \quad (\nu = 1, \dots, 2N_s). \quad (3)$$

Step 4: Average the variance functions of all  $2N_s$  segments to obtain the DFA fluctuation function,

$$F_q(s) = \left( \frac{1}{2N_s} \sum_{\nu=1}^{2N_s} (F^2(\nu, s))^{\frac{q}{2}} \right)^{\frac{2}{q}}, \quad (4)$$

where  $q$  is an integer which represents the order of DFA fluctuation function. For  $q=0$ , the DFA fluctuation function follows the formula below:

$$F_0(s) = \exp \left( \frac{1}{4N_s} \sum_{\nu=1}^{2N_s} \ln(F^2(\nu, s)) \right). \quad (5)$$

Step 5: Repeat steps 3 and 4 to obtain fluctuation functions for different segment lengths  $s$  (but no longer than  $N/4$ ). If the original time series are long-range power law-correlated, then  $F_q(s)$  increases as a power law

$$F_q(s) \sim s^{h(q)}, \quad (6)$$

which will exhibit straight lines in log-log plots.  $h(q)$  in Eq. (6) is called the generalized Hurst exponent and describes the scaling behavior of the  $q$ th order fluctuation function.  $h(q)$  describes the scaling behavior of the segments with large fluctuations for  $q>0$  and small fluctuations for  $q<0$ . For mono-fractal time series,  $h(q)$  is independent of  $q$ , whereas for multi-fractal time series,  $h(q)$  varies with  $q$  (Kantelhardt et al., 2002).

The traditional method to characterize multi-fractal series is to calculate the singularity spectrum  $f(\alpha)$  (Feder, 1988; Bunde and Havlin, 1995), which can be related to  $h(q)$  via a Legendre transform (Kantelhardt et al., 2002; Bunde and Havlin, 1995)

$$\alpha = h(q) + q \frac{dh(q)}{dq}, \quad (7)$$

$$f(\alpha) = q(\alpha - h(q)) + 1, \quad (8)$$

where  $\alpha$  is the fractal exponent, and  $f(\alpha)$  denotes the dimension of the subset of the series that is characterized by  $\alpha$ .

### 3 Multi-fractal features of daily mean relative humidity

We applied the method of MF-DFA4 in this study, which means that the trend  $P_\nu(j)$  in Eq. (2) was calculated by 4th-order polynomial fitting. MF-DFA4 was chosen because the crossovers in the log-log plots can be minimized when the order of the polynomial fitting trend up to 4th, and for an even higher order, MF-DFA can only reach similar results. Before applying the method, we remove the annual cycle of the original time series by subtracting the long-time average of the same calendar day in a year.

The fluctuation functions versus  $s$  (i.e.,  $F_q(s) \sim s^{h(q)}$ ) for the relative humidity fluctuation series with varying moments  $q$  over 191 stations were computed. Because the sample size was limited and the error would be quite large for a large  $q$ , the analysis is limited within the range of  $q = -5, -4, -3, -2, -1, 0, 1, 2, 3, 4$ , and 5. The fixed time range of 100–1000 days was chosen in the log-log plots of  $F_q(s) \sim s^{h(q)}$  to obtain  $h(q)$  for a more reasonable comparison, although the scaling range of the relative humidity fluctuations for most stations is greater than the one we chose. To estimate  $h(q)$  for  $q$  in the whole real number field, we employed the formula (Feng et al., 2010; Kantelhardt et al., 2002)

$$h(q) = \frac{1}{q} - \frac{\ln(a^q + b^q)}{q \ln 2}, \quad (9)$$

where  $a$  and  $b$  are two parameters to fit the calculated  $h(q)$ . Notice that  $h(q)$  may admit different behaviors for  $q>0$  and  $q<0$ , and thus, we fitted Eq. (9) for a range of  $q>0$  and  $q<0$ , respectively.

Figure 1a shows the  $h(q) \sim q$  of the relative humidity series for two representative stations Guangzhou (23°10'N, 113°20'E) and Kashi (39°28'N, 75°59'E) together with the well-fitted results. The multi-fractal spectra can be calculated using the fitting results together with Eqs. (7) and (8). The spectra for the representative stations are shown in Fig. 1b, where the obvious differences between two shapes reflect the different multi-fractal behaviors. Three multi-fractal parameters then can be defined: the spectrum width  $\Delta\alpha$ , the asymmetry  $\Delta\alpha_{as}$ , and the long-range correlation exponent  $\alpha_0$ , which corresponds to the peak of the singularity spectrum (Telesca et al., 2003). The results of the two representative stations are  $\Delta\alpha=0.67$ ,  $\Delta\alpha_{as}=0.01$ , and  $\alpha_0=0.89$  for Guangzhou and  $\Delta\alpha=0.22$ ,  $\Delta\alpha_{as}=0.07$ , and  $\alpha_0=0.74$  for Kashi, respectively. We then study the multi-fractal behaviors of the air relative humidity records over China according to these three parameters.

#### 3.1 $\Delta\alpha$ features

Following Eq. (9), the width of a singular spectrum is given by

$$\Delta\alpha = \alpha(-\infty) - \alpha(\infty) = \frac{\ln(b_1) - \ln(a_2)}{\ln 2}, \quad (10)$$

where  $b_1$  is the fitting coefficient for  $q<0$ , and  $a_2$  for  $q>0$ . The parameter  $\Delta\alpha$  reflects the range of singular exponents, which characterize the long-range correlations, and it reflects the strength of the multi-fractal behavior. We can

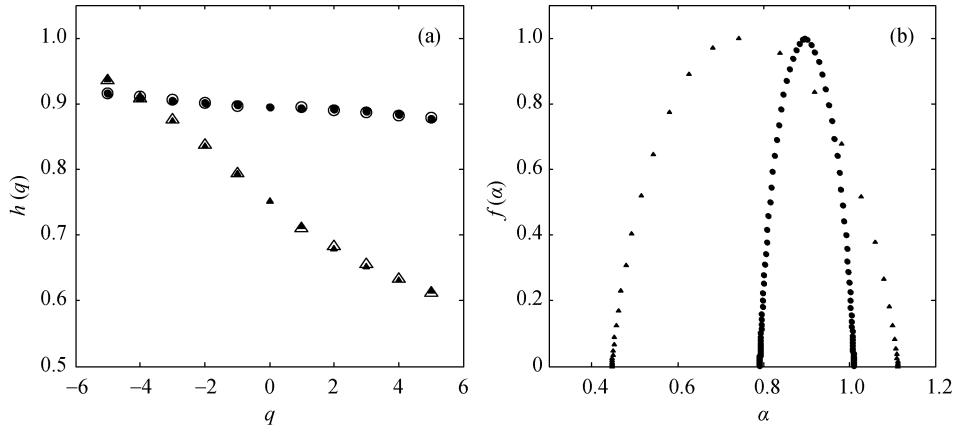


**Figure 1** (a)  $h(q)$ - $q$  curves of the relative humidity time series at two representative stations Guangzhou (triangle) and Kashi (circle). Solid icons: results from the MF-DFA of raw time series; open icons: obtained by fits of the binomial model; (b) Singularity spectra of relative humidity time series at two representative stations: Guangzhou (solid triangle) and Kashi (solid circle).

infer from Fig. 1b that the multi-fractal behavior of the relative humidity series for Guangzhou is stronger than that of Kashi.

The  $\Delta\alpha$  over the 191 stations exhibit a roughly normal distribution, with its peak at 0.3, as shown in Fig. 2a, which indicates that the relative humidity fluctuations are multi-fractal overall. Generally speaking, there are two different types of multi-fractal behavior originating in the time series: one is due to a broad probability density function for the values of the time series, and the other is due to different long-range correlations for the small and large fluctuations, which can be eliminated by shuffling the time series (Kantelhardt et al., 2002). To distinguish these two types of multi-fractal behavior, we computed  $\Delta\alpha$  following the same procedures for the shuffled relative humidity fluctuations, and the results are also shown in Fig. 2a. The  $\Delta\alpha$  dramatically decrease through the shuffling processes, and the largest  $\Delta\alpha$  is smaller than 0.3. Moreover, we found that even when shuffling the relative humidity fluctuations of a single station for many times, the  $\Delta\alpha$  could differ from each other while varying between 0 and 0.3. Therefore, we can conclude that for relative humidity records with  $\Delta\alpha < 0.3$ , their multi-fractal behavior originates from a broad distribution of the probability

density function of their values but not from properties of long-range correlation. Approximately 30%–40% of the total records lie within  $\Delta\alpha < 0.3$ ; these can be regarded as records with mono-fractal or weak multi-fractal behavior. Records with  $\Delta\alpha > 0.3$ , however, are multi-fractal and are mainly caused by different long-range correlations of the small and large relative humidity fluctuations or the complexity of physical processes that determine the variation of relative humidity in nature.

The geographic distributions of  $0.45 > \Delta\alpha > 0.3$  and  $\Delta\alpha > 0.45$  are shown in Fig. 3. Obviously, those stations with  $\Delta\alpha > 0.45$ , which indicates strong multi-fractality, are mainly distributed in southwest and small region in northwest. This concentrated geographic distribution reflects the role of climate dynamic processes on the multi-fractal behavior of relative humidity and the distinctiveness of physical processes in those regions. By analyzing the multi-fractal behavior of relative humidity, we found that for most records with the multi-fractal behavior originating from different long-range correlations of the small and large fluctuations, these behaviors are not obvious enough and can be largely characterized by a single scaling exponent. For some records in Yunnan, Guangdong, and Inner Mongolia provinces, however, the

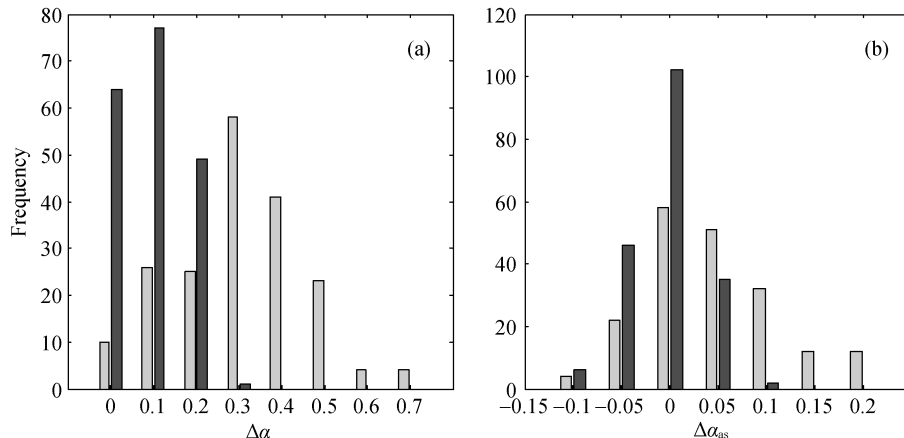


**Figure 2** Histograms of (a)  $\Delta\alpha$  and (b)  $\Delta\alpha_{as}$  of the relative humidity time series and shuffled time series at 191 stations. Gray column: raw time series; black column: shuffled time series.

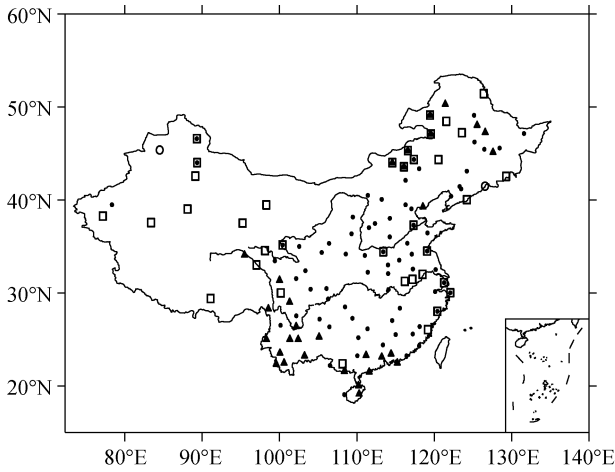


**Figure 3** Geographic distribution of  $0.3 < \Delta\alpha < 0.45$  (solid circle),  $\Delta\alpha > 0.45$  (solid triangle),  $\Delta\alpha_{as} > 0.1$  (open square), and  $\Delta\alpha < -0.1$  (open circle) for the relative humidity time series.

long-term correlations are characterized by more scaling exponents, and they have different scaling exponents for fluctuations of different amplitudes. These results are helpful to further understand regional climate prediction.

### 3.2 $\Delta\alpha_{as}$ behavior

$\Delta\alpha_{as}$  is defined as

$$\Delta\alpha_{as} = (\alpha(-\infty) - \alpha(0)) - (\alpha(0) - \alpha(\infty)), \quad (11)$$

which reflects the relative importance between the high and low fractal exponents. A positive  $\Delta\alpha_{as}$  means that the high fractal exponent is dominant and exhibits a left-skewed singularity spectrum, while a negative  $\Delta\alpha_{as}$  indicates the opposite. The asymmetry of a singularity spectrum indicates the different range sizes of scaling exponents for large and small fluctuations, which reflects the multi-fractal behavior in detail. Of course, the range size of the scaling exponents for large and small fluctuations is equal for a symmetrical singularity spectrum. The multi-fractal spectra of relative humidity in Guangzhou and Kashi are highly symmetrical, as shown in Fig. 1b.

The histograms of the  $\Delta\alpha_{as}$  of relative humidity and the corresponding shuffled series for the 191 stations are shown in Fig. 2b. We found that most singular spectra of the relative humidity records are symmetrical, as are the shuffled ones. A few, however, exhibit some asymmetry with consistently left-skewed spectra, which reflects that the long-range correlations of small fluctuations are more complex than large fluctuations, and the spectra require a larger range of scaling exponents to characterize their variation. Considering the error from the algorithm and the statistics, we chose  $\Delta\alpha_{as} > 0.1$  as the range of strong asymmetry of a singular spectrum. Figure 3 shows the geographic distribution of  $\Delta\alpha_{as} > 0.1$ , and we found that stations with a large  $\Delta\alpha_{as}$  are located in both West and East China. In the large regions between  $100^\circ\text{E}$  and  $115^\circ\text{E}$ , the singularity spectra from these stations are symmetrical, which reflects the regularity of the relative humidity fluctuations in these regions.

### 3.3 $\alpha_0$ characteristics

According to Eq. (7),  $\alpha_0 = h(0)$  is the generalized Hurst exponent for  $q=0$ , and it characterizes the long-term correlation of normal fluctuations with the amplitude between large and small fluctuations and reflects the basic level of all long-range correlations: the larger  $\alpha_0$  is, the stronger the long-range correlations of the fluctuations. In fact, the long-range correlation exponents are linearly correlated with those derived from DFA, exhibiting a line in the  $\alpha_0 \sim \alpha$  plots (Fig. 4).

The geographic distribution of  $\alpha_0$  for the relative humidity time series (Fig. 5) exhibits a larger  $\alpha_0$  in northern China in general and relatively smaller  $\alpha_0$  in southern China, which indicates a stronger long-range correlation and better predictability in northern China. It should be noted that for a shuffled time series,  $\alpha_0$  is approximately 0.5, which is identical to the Hurst exponent for white noise, because the related structure was removed by the shuffling processes.

Based on the results above, we found that through the shuffling processes,  $\Delta\alpha$  and  $\Delta\alpha_{as}$  are prone to 0 and  $\alpha_0$  to

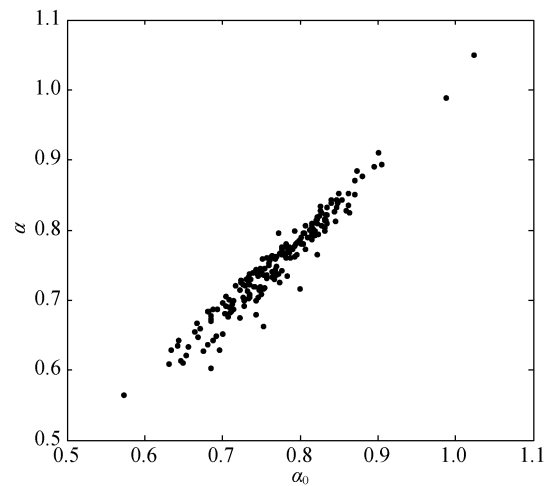


**Figure 4**  $\alpha_0 \sim \alpha$  plots of the relative humidity time series at 191 stations.

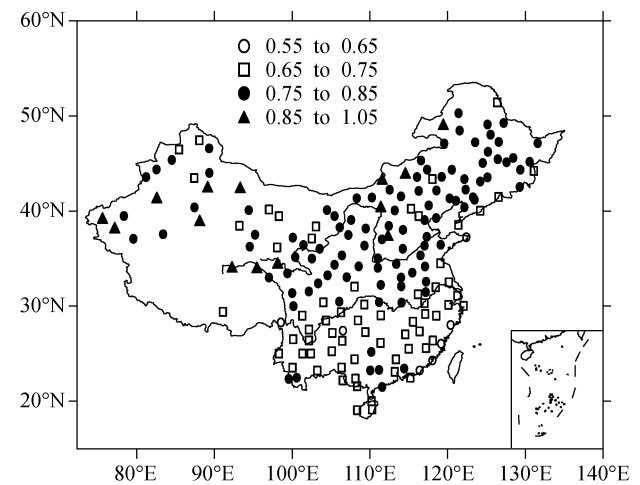


**Figure 5** Geographic distribution of  $\alpha_0$  of the relative humidity time series at 191 stations.

0.5. Therefore, every specified status of  $\Delta\alpha$ ,  $\Delta\alpha_{as}$ , and  $\alpha_0$  reflects the characteristics of the corresponding records' structure, and they are useful to study the future evolution features in specific processes.

#### 4 Conclusions

In this paper, the MF-DFA method was applied to study the multi-fractal behaviors of daily average relative humidity records over China. By studying three multi-fractal parameters ( $\Delta\alpha$ ,  $\Delta\alpha_{as}$ , and  $\alpha_0$ ) of a singularity spectrum, we found that multi-fractal behavior exists in relative humidity records at most stations in China, mainly due to the broad distribution of sequence values. For some stations in Yunnan, Guangdong, and Inner Mongolia provinces, the multi-fractal behaviors are much stronger and are mainly caused by different long-range correlations between large and small fluctuations, which result in more complicated predictability in these regions. The asymmetry of the singularity spectra of the relative humidity records is weak except for a small number of stations in far eastern and western China. The singularity spectra are left-skewed in those stations, which means the long-range correlations of small fluctuations are more complicated than large fluctuations, and the small fluctuations need more scaling exponents to be characterized. For the stations between 100°E and 115°E, the singularity spectra are symmetrical, which reflects the regularity of the relative humidity fluctuations in the regions. The long-range correlations in northern China are stronger than those of southern China, which indicates better predictability in northern China. The three multi-fractal parameters describe the long-term correlations from different views, and a specified combination of them represents a particular long-range correlation of the corresponding processes. These results are helpful to fully understand the long-range correlations of relative humidity records and may provide theoretical support in climate prediction.

**Acknowledgements.** This research was supported by the National Natural Science Foundation of China (40975027).

#### References

- Bunde, A., and S. Havlin, 1995: *Fractals in Science*, Springer-Verlag, Berlin, 298pp.
- Bunde, A., and S. Havlin, 2002: Power-law persistence in the atmosphere and in the oceans, *Physica A*, **314**, 15–24.
- Chen, H., and S. C. Guo, 1997: The multifractal characteristics of climate change at Kunming, *Climatic Environ. Res.* (in Chinese), **2**(4), 361–368.
- Chen, X., G. X. Lin, and Z. T. Fu, 2007: Long-range correlations in daily relative humidity fluctuations: A new indexes to characterize the climate regions over China, *Geophys. Res. Lett.*, **34**, L07804, doi:10.1029/2006GL027755.
- Feder, J., 1988: *Fractals*, Plenum Press, New York, 90pp.
- Feng, T., Z. T. Fu, and J. Y. Mao, 2010: The multi-fractal characteristics of climate variables in Beijing, *Chinese J. Geophys.* (in Chinese), **53**(9), 2037–2044.
- Fraedrich, K., and R. Blender, 2003: Scaling of atmosphere and ocean temperature correlations in observations and climate models, *Phys. Rev. Lett.*, **90**, 108501, doi:10.1103/PhysRevLett.90.108501.
- Guo, S. C., Y. L. Chang, H. Chen, et al., 2004: The multifractal characteristics of climate change in Yunnan, China, *J. Yunnan University* (in Chinese), **26**(4), 325–330.
- Jiang, T. H., and L. T. Deng, 2004: Multifractal spectra of global temperature, *J. Trop. Meteor.* (in Chinese), **20**(6), 673–678.
- Kantelhardt, J. W., S. A. Zschiegner, E. Koscielny-Bunde, et al., 2002: Multi-fractal detrended fluctuation analysis of nonstationary time series, *Physica A*, **316**, 87–114.
- Kantelhardt, J. W., E. Koscielny-Bunde, H. A. Rego, et al., 2001: Detecting long-range correlations with detrended fluctuation analysis, *Physica A*, **295**, 441–454.
- Koscielny-Bunde, E., A. Bunde, S. Havlin, et al., 1998: Indication of a universal persistence law governing atmospheric variability, *Phys. Rev. Lett.*, **81**, 729–732.
- Lin, G. X., X. Chen, and Z. T. Fu, 2007: Temporal-spatial diversities of long-range correlation for relative humidity over China, *Physica A*, **383**, 585–594.
- Liu, S. D., 1990: Earth system modeling and chaotic time series, *Chinese J. Geophys.* (in Chinese), **33**(2), 144–153.
- Shi, S. Y., S. D. Liu, Z. T. Fu, et al., 2005: The characteristic analysis of weather and climate time series, *Chinese J. Geophys.* (in Chinese), **48**(2), 259–264.
- Telesca, L., G. Colangelo, V. Lapenna, et al., 2003: Monofractal and multifractal characterization of geoelectrical signals measured in southern Italy, *Chaos, Solitons and Fractals*, **18**, 385–399.
- Talkner, P., and R. O. Weber, 2000: Power spectrum and detrended fluctuation analysis: Application to daily temperatures, *Phys. Rev. E*, **62**, 150–160.
- Vattay, G., and A. Harnos, 1994: Scaling behavior in daily air humidity fluctuations, *Phys. Rev. Lett.*, **73**, 768–771.
- Zhai, P. M., and X. H. Pan, 2003: Trends in temperature extremes during 1951–1999 in China, *Geophys. Res. Lett.*, **30**, 1913, doi:10.1029/2003GL018004.
- Zhai, P. M., X. B. Zhang, H. Wan, et al., 2004: Trends in total precipitation and frequency of daily precipitation extremes over China, *J. Climate*, **18**, 1096–1107.
- Zou, X. K., P. M. Zhai, and Q. Zhang, 2005: Variations in droughts over China: 1951–2003, *Geophys. Res. Lett.*, **32**, L04707, doi:10.1029/2004GL021853.